Single Molecule Conductance of Bipyridyl Ethynes The Role of Surface Binding Modes

ARTICLE *in* THE JOURNAL OF PHYSICAL CHEMISTRY B · NOVEMBER 2009

Impact Factor: 3.3 · DOI: 10.1021/jp9083579 · Source: PubMed

Single Molecule Conductance of Bipyridyl Ethynes: The Role of Surface Binding Modes[†]

Kirill A. Velizhanin,[‡,§] Tarek A. Zeidan,[||,⊥] Igor V. Alabugin,[||] and Sergei Smirnov*[,‡]

Department of Chemistry and Biochemistry, New Mexico State University, Las Cruces, New Mexico 88003, and Department of Chemistry, Florida State University, Tallahassee, Fl 32306

Received: August 29, 2009; Revised Manuscript Received: October 17, 2009

We report on the experimental studies of single molecule conductance of 1,2-bi(pyridin-4-yl)ethyne (BPY-EY) and perfluoro-1,2-bi(pyridin-4-yl)ethyne (PFBPY-EY). The conductance measurements of the molecules bridging two Au electrodes have been carried out in toluene solutions using the scanning tunneling microscopy (STM) based break junction technique. Two conductance values of $(2.2 \pm 0.5) \times 10^{-4}$ and $(5.0 \pm 0.8) \times 10^{-5}$ G_0 have been found for BPY-EY but only one, $(4.2 \pm 0.5) \times 10^{-5}$ G_0, for PFBPY-EY. The disparity is attributed to steric differences between the molecules at the electrode.

Introduction

Studies of charge transfer for single molecules in metal−molecule−metal (MMM) junctions have intensified recently both in number of experiments and in theoretical methods (see, e.g., refs 1−5 and references therein). The interest is driven, among other things, by the search for novel miniaturized and fast electronic components that would comply with demands of Moore's law.[6] This quest naturally leads to molecules as the ultimate elementary building blocks of future subnanometer sized electronic components.

Many intriguing phenomena taking place in MMM junctions are yet to be carefully studied and understood before the practical realization of molecular electronic devices could be attempted. One of such phenomena is the effect of metal−molecule contact on the properties of an MMM device. It was found that the molecular conductance is influenced not only by the choice of the anchoring group, −SH, $-NH_2$, −COOH, pyridyl, or others, but also by the specific orientation of the group relative to the surface at the contact. Differences in the orientations can modify alignment of the molecule and result in more than one molecule's conductance.[7−14] The latter effect is especially crucial in applications of MMM devices.

In this paper, we report our results on measuring the conductance of two 4,4′-bipyridyl ethynes, unsubstituted BPY-EY and perfluorinated PFBPY-EY. The possibility of different Au−molecule contact geometries and their dependence on the molecular structure is discussed. Two Au−molecule contact geometries were observed for BPY-EY as two sets of molecular conductance, in agreement with previous reports, while only a single conductance was detected for fluorinated PFBPY-EY, which is explained by differences in the contact geometry for the latter substrate with Au. Possible consequences of this interpretation are discussed.

Experimental Section

Au(111) on mica substrates and gold STM tips were employed to construct the Au−molecule−Au junctions. Prior to each experiment, the Au substrate was annealed in a hydrogen flame. The Au tip was prepared from a 0.25 mm gold wire (Alfa Aesar, 99.998%) by the cutting−pulling method,[15] which, due to mechanical properties of gold, leads to a nearly atomic sharpness. The synthesis of BPY-EY and PFBPY-EY compounds is described elsewhere.[16]

The conductance measurements were carried out on a Molecular Imaging STM (Molecular Imaging, US) modified with the capability for external computer control of *z*-piezo movement. A Teflon STM cell was cleaned prior to every experiment by Piranha solution (98% H_2SO_4:30% H_2O_2 = 3:1 by volume) and then washed with copious amounts of ultrapure DI water. For each molecule under study, its solution in the highest purity toluene (Aldrich) with a typical concentration of 1 mM was placed in the STM cell under ambient conditions. Each experiment started with topographic STM imaging of the Au(111) surface in solution to find a large terrace identified by sharp monatomic steps at its perimeter. Then, the standard STM feedback was turned off and the control of the tip movement in the *z*-direction was switched over to an external computer workstation. Under the control of a LabVIEW-based program, the tip was repeatedly driven toward the substrate until the current reached a preset value corresponding to a conductance of several G_0, where $G_0 = 2e^2/h$ (≈12.9 kOhm) is the quantum of electric conductance, and then retracted from the surface at a constant speed (typically 20−50 nm/s). The current−distance curves were recorded at a sampling frequency of 20 kHz. The retraction was stopped once the tunneling current reached a comparable with the preamplifier's noise level. Typically, a few thousands of current−distance curves were collected for a single value of bias. After rejection of the current−distance curves lacking clear stepwise features, the histogram was constructed by counting the number of data points at each small current range (histogram bin). This procedure was analogously repeated for several values of bias voltage in order to reconstruct the current−voltage (*I*−*V*) characteristics. The preamplifier setting was tuned to a suitable conductance range. The overall range for investigated conductance values spans from 5×10^{-6} to 10^{-3} G_0.

[†] Part of the "Michael R. Wasielewski Festschrift".

* To whom correspondence should be addressed. E-mail: snsm@nmsu.edu.
[‡] New Mexico State University.
[§] Current address: Center for Nonlinear Studies (CNLS) and T-4, Theoretical Division, Los Alamos National Laboratory, Los Alamos, NM 87545.
[||] Florida State University.
[⊥] Current address: Alkermes Inc., Cambridge, MA 02139.

10.1021/jp9083579
Published on Web 11/13/2009

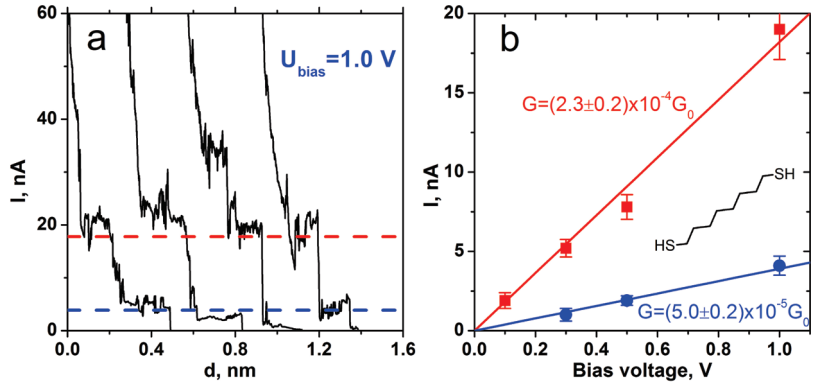

Figure 1. (a) Current−distance curves of Au−1,8-octanedithiol−Au demonstrate two series of conductance values simultaneously. The curves shown were recorded at 1.0 V bias. Statistical analysis of such curves at several values of bias voltage produces the two $I-V$ characteristics depicted by red squares (high conductance) and blue circles (low conductance) in panel b. Linear fitting of these $I-V$ curves (solid lines in panel b) produces the single molecule conductance values of $(5.0 \pm 0.2) \times 10^{-5}$ and $(2.3 \pm 0.2) \times 10^{-4}$ G_0. Each value is depicted by the corresponding current as a dashed line in panel a.

Results and Discussion

1. Conductance of Au−1,8-Octanedithiol−Au Junction. To test the performance of our experimental setup, we have measured the conductance of 1,8-octanedithiol single molecules bridging the Au(111) substrate and an STM tip. This system has become a standard experiment for calibration and verification in the break junction experiments.

It has been reported by several groups that Au−1,8-octanedithiol−Au MMM junctions can have more than one conductance value,[7,17,18] which was tentatively attributed to two possible geometries of the contact between thiol groups and gold. Specifically, the "top" geometry is believed to be realized when a sulfur atom sits atop a gold atom or an adatom pulled out of the surface during the formation of an atomic gold wire. The geometry of the second, "hollow", orientation is still a matter of controversy but is believed to involve more than one gold atom at the contact. It may correspond to a sulfur atom sitting in the void between three Au atoms,[7] at a step edge, or close to gold adatoms of the substrate or the tip.[13] The two contact geometries lead to three possible conductance values for a symmetric molecule, corresponding to top−top, top−hollow, and hollow−hollow MMM geometries. The last MMM geometry has not been observed experimentally presumably due to the low probability of realization, whereas the other two have been measured to have conductance values of 5.2×10^{-5} and 2.5×10^{-4} G_0, respectively.[7]

Our measurements also result in the two sets of conductance values for this system. Figure 1a demonstrates them both as stepwise features in the current−distance curves for one bias voltage (1.0 V). The statistical weight of curves with both features was rather low (<5%), with most of the curves being either featureless (∼50−60%) or showing only steps corresponding to one conductance value, either low (top−top) (∼20%) or high (top−hollow) (∼10%). The statistical analysis of a few thousand conductance−distance curves collected at different biases resulted in the two $I-V$ characteristics shown in Figure 1b. These $I-V$ curves demonstrate visible nonlinear behavior for biases beyond 1 V, but within the range presented on the graph, the nonlinearity is negligible. Linear fitting of the $I-V$ curves yielded two conductance values, $(5.0 \pm 0.2) \times 10^{-5}$ and $(2.3 \pm 0.2) \times 10^{-4}$ G_0, which agree with the previously reported results. Existence of curves possessing both the high and the low conductance features as well as a higher probability of the latter do not necessarily suggest that the lower conductance top geometry is thermodynamically more favorable but rather illustrate that even initially anchored in the hollow geometry molecules can be pulled up before breaking off.

2. Conductance of BPY-EY and PFBPY-EY. Similar data were collected for BPY-EY and PFBPY-EY, also in 1 mM toluene solutions. Typical current−distance curves containing stepwise features and the constructed current histograms for BPY-EY and PFBPY-EY are shown in Figures 2 and 3, respectively. Each histogram was constructed from 2000−3000 current−distance curves. The well pronounced peaks in the histograms are interpreted as corresponding to the tunneling current through an integer number of molecules sandwiched between the gold substrate and the STM tip. The histograms are rather noisy and rarely display well-identifiable two- or three-molecule peaks. In order to improve the accuracy and eliminate false-reading, the histograms were collected for several bias voltages, which brought the total number of analyzed current−distance curves to well over 10 000 for each conductance range. Erroneous peaks occasionally appearing on the histograms (Figures 2 and 3) but failing to reproduce at all biases were discarded. Thus obtained $I-V$ dependences for the two molecules of interest are depicted in Figure 4 and suggest that there are two conductance values for BPY-EY, $(2.2 \pm 0.5) \times 10^{-4}$ and $(5.0 \pm 0.8) \times 10^{-5}$ G_0, while only one value of $(4.2 \pm 0.5) \times 10^{-5}$ G_0 is measured for fluorinated PFBPY-EY. The statistical weights of the lower conductance value of BPY-EY and the only conductance value of PFBPY-EY were found to be similar, ∼25% of all the current−distance curves. In contrast, the higher conductance value of BPY-EY was of a noticeably lower statistical weight (∼6% of all the current−distance curves).

BPY-EY is expected to be similar to the 4,4′-bipyridine molecule (BPY) with respect to possible geometries of molecule−metal contacts. Recently, two sets of conductance values for BPY were observed by two groups.[12,19] Similar to the case of 1,8-octanedithiol, the two conductance values were attributed to different binding geometries. Specifically, Zhou et al.[19] reported the conductance values of 4.7×10^{-3} and 5.9×10^{-4} G_0, but Quek et al.[12] reported the conductance values of 6×10^{-4} and 1.6×10^{-4} G_0. Notably, the lower conductance value measured by Zhou et al. is very close to the higher one measured by Quek et al. Furthermore, the latter group observed the high conductance tail extending to $\sim 3 \times 10^{-3}$ G_0, approximately where the higher conductance value of 4.7×10^{-3} G_0 was observed by Zhou et al. Therefore, the apparent discrepancy between the observations of these two groups can

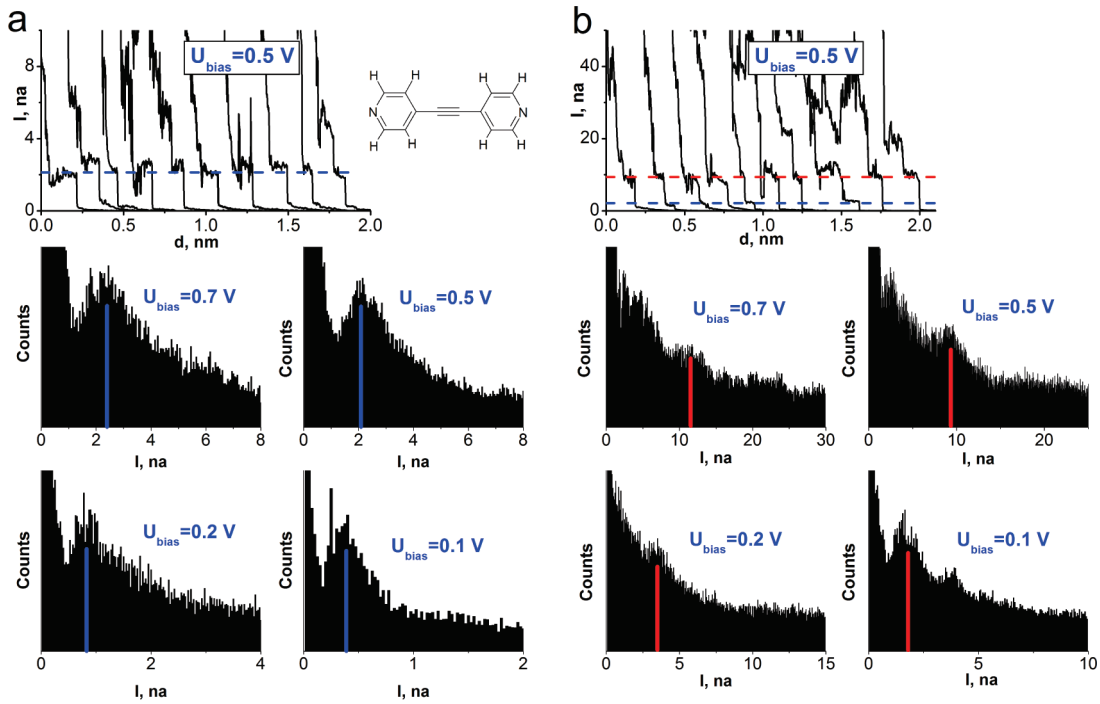

Figure 2. Typical current−distance curves with stepwise features (top plots) and the current histograms at different values of bias for BPY-EY. The current−distance curves were recorded at 0.5 V bias. Panels a and b correspond to the lower and higher conductance values, respectively. The values of current extracted from histograms are depicted as colored vertical solid and horizontal dashed lines in the histogram and current−distance plots, respectively (color code: blue, lower conductance; red, higher conductance).

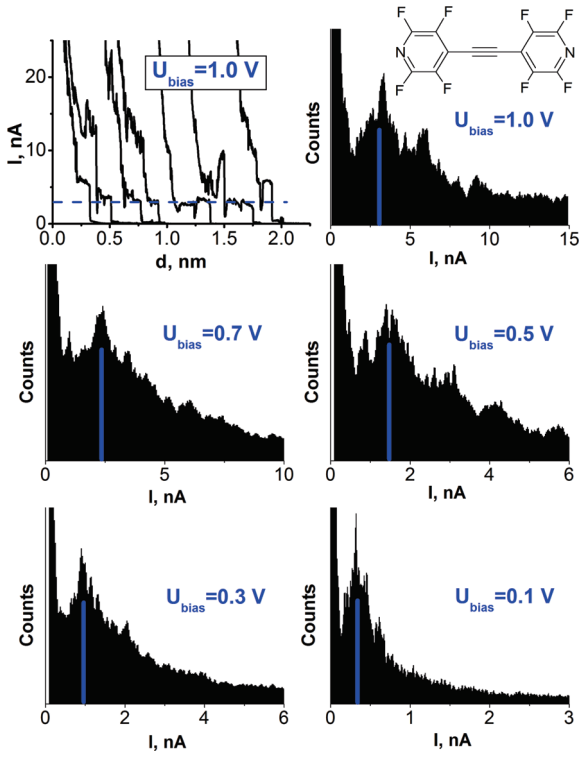

Figure 3. Typical current−distance curves with stepwise features (the top left plot at 1.0 V bias) and the current histograms at different values of bias for PFBPY-EY. The values of current extracted from histograms are depicted as blue lines (horizontal dashed in the current−distance plot and vertical solid in the histogram plots).

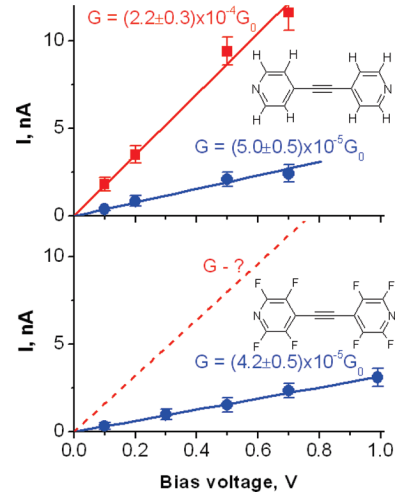

Figure 4. *I*−*V* dependences for BPY-EY (top panel) and PFBPY-EY (bottom panel) molecules. The "missing", i.e., not observed experimentally, conductance for PFBPY-EY is illustrated by the dashed line.

be circumvented by assuming that there are three distinct conductance values for BPY: 4.7×10^{-3}, $\sim 6 \times 10^{-4}$, and 1.6×10^{-4} G_0. Then, observations by Quek et al. are providing the lower conductance pair, while Zhou et al. observed the pair with higher conductances.

Zhou et al.[19] also measured the conductances of bipyridyl ethene (BPY-EE), 2.3×10^{-3} and 2.4×10^{-4} G_0. Comparison of these values to the top two conductances of BPY gives a 2−2.5-fold decrease of conductance upon insertion of an ethene group (CH═CH) in between the pyridine moieties. Applying this empirical factor to the third (lowest) conductance value of BPY, 1.6×10^{-4} G_0, one should expect the remaining third conductance of BPY-EE on the order of $(6-8) \times 10^{-5}$ G_0. This value combined with the lower one found by Zhou et al. for the same molecule is close but slightly higher than what we have found for BPY-EY, 2.2×10^{-4} and 5×10^{-5} G_0. Such differences are expected, since the ethyne moiety C≡C in BPY-EY affects both molecular length and electronic structure: BPY-EY is longer than BPY-EE and the highest occupied molecular

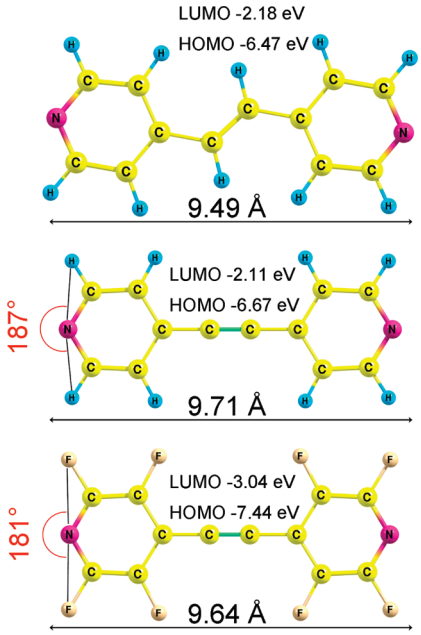

Figure 5. Optimized ground state geometries and energies of frontier orbitals for BPY-EE (top), BPY-EY (middle), and PFBPY-EY (bottom). Molecular length is defined as the distance between nitrogen atoms. The density functional theory calculations were performed using the B3LYP hybrid functional and 6-31G* basis set (using the Gaussian 03 *ab initio* quantum chemistry package[20]).

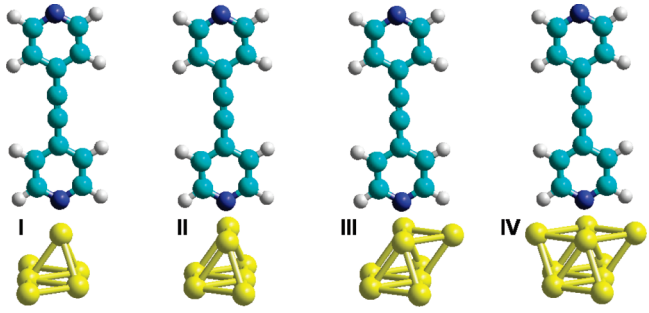

Figure 6. Top (I) and hollow (II−IV) contact geometries for the BPY-EY molecule.

orbital (HOMO) of BPY-EY is lower by ∼0.2 eV (see Figure 5 for details). These correlations suggest that the two observed conductances of BPY-EY represent the lower pair out of the possible three. Similar to Quek et al.,[12] we did not see the highest conductance value.

The possible geometries of molecule−metal contacts for pyridine anchoring groups were addressed in recent studies using BPY.[12,21] Similar to the case of 1,8-octanedithiol, it was concluded that at each molecular end either a "top" (lower conductance) or a "hollow" (higher conductance) contact geometry can be realized. Therefore, one can conclude the following: (a) Quek et al.[12] measured the BPY conductances corresponding to top−top and top−hollow geometries. (b) Zhou et al.[19] saw top−hollow and hollow−hollow geometries. Finally, (c) we measured the top−top and top−hollow conductances of BPY-EY. Similar to the case of 1,8-octandedithiol, in the top geometry, nitrogen's lone pair is coordinating directly onto one Au atom (see structure I in Figure 6), while the hollow geometry is less apparent with some possible examples shown in Figure 6 (II−IV). It was suggested that the hollow geometry is sterically unfavorable due to repulsion between gold and ortho hydrogen atoms of the pyridine moiety.[21] This notion is supported by our observation of the lower statistical weight for the higher conductance value of BPY-EY.

It is strikingly different that we observe only one conductance value for fluorinated PFBPY-EY, $(4.2 \pm 0.5) \times 10^{-5}$ G_0. The value is close to the lowest conductance of BPY-EY and thus most likely corresponds to the top−top MMM geometry. Note that this conductance is lower than the corresponding one of BPY-EY, which can be justified by previously suggested HOMO tunneling in similar molecules.[22] Indeed, the HOMO of PFBPY-EY is nearly 0.8 eV lower, according to our DFT calculations (see Figure 5). Besides, if it were the high-conductance top−hollow MMM geometry, it would imply that there is another low-conductance value for PFBPY-EY that should be realized with a higher statistical weight as for BPY-EY. However, no such conductance was observed experimentally.

The absence of a higher conductance value for PFBPY-EY calls for further analysis of the contact geometry. As discussed above, the hollow binding in the case of BPY (and BPY-EY) is unfavorable due to steric repulsion. The results of density functional theory calculations, Figure 5, show that ortho fluorines in PFBPY-EY stick out farther than the corresponding hydrogens in BPY-EY: the F−N−F angle of 181° is smaller than the corresponding H−N−H angle of 187°, and the larger van der Waals radius of fluorine further emphasizes the effect. Therefore, the hollow type of pyridyl attachment to the surface may be even more hindered in the fluorinated case.

The exact geometry of the hollow configuration is unknown, and different possibilities have been discussed.[12,21,23] In Figure 6, we schematically represented a simplistic discrimination between them as coordination by two (II), three (III), and four (IV) Au atoms. It has been argued that the higher conductance of the hollow contact geometry may be due to a greater coupling between the molecule's π-system and the substrate, which is achieved when the nitrogen is coordinated *between* two Au atoms (see II in Figure 6). Since no hindrance from ortho hydrogens (fluorines) is apparent in such a geometry, we have to conclude that the probability of such a metal contact is rather low. Because configurations with three and four Au atoms (III and IV in Figure 6) would have to experience that hindrance, they are more likely to occur under the experimental conditions. In both cases III and IV, additional hindrance is caused by farther extended ortho fluorines and would practically prevent the realization of hollow contacts in the case of PFBPY-EY. Pluchery et al.[23] concluded from DFT calculations for pyridyls on Au(111) surfaces that the top geometry is almost 0.5 eV more stable than the hollow geometries, justifying its higher statistical weight in our experiments. As in the case of dithiols, such a statistical bias toward the lower conductance values can be also enhanced by a nonzero probability of pulling a molecule from the hollow geometry to the top.

One can probably suggest an alternative assignment to the conductance and argue that two ortho fluorine atoms in fact participate in coordination by gold atoms even at the expense of weakening the interaction with nitrogen. Such attractive F···Au interaction would lead to a three-prong coordination mode and formation of a favored well-defined binding geometry which may also account for the single conductance value. Due to the lack of quantitative data on the magnitude of Au···F interactions, currently there is no sufficient experimental information to unequivocally reject this alternative, but as mentioned above, the top geometry should have no restriction for realization unless it is too unstable. Moreover, we corroborate our assignment because such anchoring with fluorines would likely lead to an increase above the higher conductance value

(as due to hollow geometry) and not to the experimentally observed value which is less than the lower conductance value (of the top geometry) for regular BPY-EY.

It is important to note that the top geometry of the contact is not limited exclusively to the one presented in I of Figure 6, where a single Au atom is terminating the surface. A BPY-EY molecule in a hollow configuration upon pulling can and does often end up in the top geometry.

Steric hindrance, which prevents formation of the hollow geometry of PFBPY-EY binding to gold, can be applied in designing well-defined molecular junctions on gold, where only one geometry of the contacts is realized. Employment of other ortho substituents such as methyls can be used to verify whether the top geometry is actually realized on a pulled away single Au atom or an atom surrounded by a few more atoms.

Conclusion

We have measured the single molecule conductance of bipyridyl ethyne (BPY-EY) and its perfluorinated analogue (PFBPY-EY) at different bias voltages. BPY-EY shows two sets of conductance values, $(2.2 \pm 0.5) \times 10^{-4}$ G_0 for the hollow and $(5.0 \pm 0.8) \times 10^{-5}$ G_0 for the top molecular junction geometry, respectively, while PFBPY-EY demonstrates only the top junction with a conductance of $(4.2 \pm 0.5) \times 10^{-5}$ G_0. The absence of the hollow contact configuration in the latter case is due to a greater steric hindrance from CF bonds vicinal to nitrogens coordinating onto the Au(111) surface. This finding opens an opportunity for designing well-defined molecular junctions on gold.

Acknowledgment. The authors gratefully thank Dr. Nongjian Tao, Dr. Bingqian Xu, and Dr. Joshua Hihath of Arizona State University for the fruitful and stimulating discussions. This work was partially supported by a grant from the National Institutes of Health (NIH SCORE GM08136). Work at FSU is supported by the National Science Foundation (CHE-0848686).

References and Notes

(1) Nitzan, A. *Annu. Rev. Phys. Chem.* **2001**, *52*, 681.
(2) Nitzan, A.; Ratner, M. A. *Science* **2003**, *300*, 1384.
(3) Mantooth, B. A.; Weiss, P. S. *Proc. IEEE* **2003**, *91*, 1785.
(4) Chen, F.; Hihath, J.; Huang, Z.; Li, X.; Tao, N. J. *Annu. Rev. Phys. Chem.* **2007**, *58*, 535.
(5) Tao, N. J. *Nat. Nanotechnol.* **2006**, *1*, 173.
(6) Moore, G. E. *Electronics* **1965**, *38*, 8.
(7) Li, X.; He, J.; Hihath, J.; Xu, B. Q.; Lindsay, S. M.; Tao, N. J. *J. Am. Chem. Soc.* **2006**, *128*, 2135.
(8) Chen, F.; Li, X.; Hihath, J.; Huang, Z.; Tao, N. J. *J. Am. Chem. Soc.* **2006**, *128*, 15874.
(9) Tsutsui, M.; Teramae, Y.; Kurokawa, S.; Sakai, A. *Appl. Phys. Lett.* **2006**, *89*, 163111.
(10) Kristensen, I. S.; Mowbray, D. J.; Thygesen, K. S.; Jacobsen, K. W. *J. Phys: Condens. Matter* **2008**, *20*, 374101.
(11) Gonzales, M. T.; Brunner, J.; Huber, R.; Wu, S.; Schonenberger, C.; Calame, M. *New J. Phys.* **2008**, *10*, 076028.
(12) Quek, S. Y.; Kamenetska, M.; Steigerwald, M. L.; Choi, H. J.; Louie, S. G.; Hybertsen, M. S.; Neaton, J. B.; Venkataraman, L. *Nat. Nanotechnol.* **2009**, *4*, 230.
(13) Haiss, W.; Martín, S.; Leary, E.; van Zalinge, H.; Higgins, S. J.; Bouffier, L.; Nichols, R. J. *J. Phys. Chem. C* **2009**, *113*, 5823.
(14) Zhou, J. F.; Chen, F.; Xu, B. Q. *J. Am. Chem. Soc.* **2009**, *131*, 10439.
(15) NanoSurf Operating Instructions, easyScan E-STM Version 2.1. January 2004, NanoSurf AG, Switzerland.
(16) Zeidan, T. A.; Kovalenko, S. V.; Manoharan, M.; Clark, R. J.; Chiviriga, I.; Alabugin, I. V. *J. Am. Chem. Soc.* **2005**, *127*, 4270.
(17) He, J.; Sankey, O.; Lee, M.; Tao, N. J.; Li, X.; Lindsay, S. *Faraday Discuss.* **2006**, *131*, 145.
(18) Morita, T.; Lindsay, S. *J. Am. Chem. Soc.* **2007**, *129*, 7262.
(19) Zhou, X.-S.; Chen, Z.-B.; Liu, S.-H.; Jin, S.; Liu, L.; Zhang, H.-M.; Xie, Z.-X.; Jiang, Y.-B.; Mao, B.-W. *J. Phys. Chem. C* **2008**, *112*, 3935.
(20) Frisch, M. J.; et al. *Gaussian 03*, revision B.03; Gaussian, Inc.: Wallingford, CT, 2004.
(21) Pérez-Jiménez, Á. J. *J. Phys. Chem. B* **2005**, *109*, 10052.
(22) Venkataraman, L.; Park, Y. S.; Whalley, A. C.; Nuckolls, C.; Hybersten, M. S.; Steigerald, M. L. *Nano Lett.* **2007**, *7*, 502.
(23) Pluchery, O.; Tadjeddine, M.; Flamentc, J.-P.; Tadjeddine, A. *Phys. Chem. Chem. Phys.* **2001**, *3*, 3343.

JP9083579